An analytical model for stress-induced anisotropy of a cracked solid

Boris Gurevich, Curtin University of Technology and CSIRO Earth Science and Resource Engineering*
Marina Pervukhina, CSIRO Earth Science and Resource Engineering

Summary

One of the main causes of azimuthal anisotropy in sedimentary rocks is anisotropy of tectonic stresses in the earth's crust. In this paper we analytically derive the pattern of seismic anisotropy caused by application of a small anisotropic stress. We first consider an isotropic elastic medium (porous or non-porous) permeated by a distribution of discontinuities with random (isotropic) orientation (such as randomly oriented compliant grain contacts or cracks). Geometry of individual discontinuities is not specified. Instead, their behaviour is defined by a ratio *B* of the normal to tangential excess compliances.

When this isotropic rock is subjected to a small compressive stress (isotropic or anisotropic), the density of cracks along a particular plane is reduced in proportion to the normal stress traction acting on that plane. In particular, if the stress is a uniaxial compression along the *x* axis, then the density of cracks normal to *x* axis will reduce most, while the density of cracks parallel to *x* axis will not reduce at all. This effect is modelled using Sayers-Kachanov (1995) non-interactive approximation. The results of this derivation show that such anisotropic crack closure yields elliptical anisotropy, regardless of the value of the compliance ratio *B*. It also predicts the ratio of anisotropy parameters ε / γ as function of the compliance ratio *B* and Poisson's ratio of the unstressed rock. These results are useful for differentiating stress-induced anisotropy from fracture-induced anisotropy. Conversely, if the cause of anisotropy is known, then the anisotropy pattern allows one to estimate P-wave anisotropy from S-wave anisotropy.

Introduction

One of the main causes of azimuthal anisotropy in sedimentary rocks is anisotropy of tectonic stresses in the earth's crust. Stresses affect elastic properties of rocks due to presence of discontinuities such as cracks and compliant grain contacts. Non-hydrostatic stress can cause elastic anisotropy since the effect of a stress field on a discontinuity depends on the orientation of the discontinuity with respect to the stress field. Knowledge of the pattern of stress-induced anisotropy (as expressed, for example, by the ratio of anisotropy parameters) can be useful for distinguishing it from other causes of anisotropy, such as presence of aligned fractures. Such patterns can also be used to distinguish, say, P-wave anisotropy from S-wave anisotropy estimated from S-wave splitting.

A number of authors have modeled stress-induced anisotropy by assuming the rock to contain a distribution of penny-shaped cracks, and considering variation of this distribution due to applied stress (see e.g., Nur, 1971, Sayers, 1988). However, penny-shaped crack geometry may not give an adequate quantitative description of discontinuities in rocks (Sayers and Han, 2002; Gurevich et al., 2009; Angus et al., 2009). Alternatively, Mavko et al. (1995) and Sayers (2002) developed modeling approaches that do not restrict the shape of discontinuities but instead infer their parameters from measurements. These approaches require numerical calculations to obtain an insight into anisotropy patterns.

To obtain a more simple and general insight to these patterns, we make some simplifying assumptions that allow us to compute the anisotropy parameters analytically. Our main assumption is that a rock containing an (initially) isotropic distribution of discontinuities is subjected to a *small* uniaxial stress (or uniaxial strain) such that it results in a *weak* anisotropy of the discontinuity orientation distribution, and *weak* elastic anisotropy.

Compliance tensor of a cracked solid

We first consider an isotropic elastic medium (porous or non-porous). We then assume that this medium at ambient stress is permeated by a distribution of cracks with random (isotropic) orientation. For instance, in a granular rock, these cracks may represent randomly distributed and randomly oriented compliant grain contacts. The exact geometry of individual cracks is not specified. Instead, the behaviour of cracks is defined by a ratio *B* of the normal B_N to tangential B_T excess crack compliances. All cracks are assumed identical; thus *B* is the same for all cracks.

When this isotropic rock is subjected to a small compressive stress (isotropic or anisotropic), the density of cracks along a particular plane is reduced in proportion to the normal stress traction acting on that plane. In particular, if the stress is a uniaxial compression along the *x* axis, then the density of cracks normal to *x* axis will reduce most, while the density of cracks parallel to *x* axis will not reduce at all. This effect can be modelled using Sayers-Kachanov (1995) non-interactive approximation. Specifically, the change of the compliance tensor S_{ijkl} due to application of a small anisotropic stress can be written as

$$S_{ijkl} = S^0_{ijkl} + \overline{\alpha}_{ijkl} + \beta_{ijkl}. \qquad (1)$$

with

A model for stress-induced anisotropy

$$\bar{\alpha}_{ijkl} = \frac{1}{4}\left(\delta_{ik}\alpha_{jl} + \delta_{il}\alpha_{jk} + \delta_{jk}\alpha_{il} + \delta_{jl}\alpha_{ik}\right) \quad (2)$$

Here, S^0_{ijkl} is compliance tensor of the intact rock (no cracks), α_{ij} and β_{ijkl} are second and fourth-rank tensors defined by

$$\alpha_{ij} = \frac{1}{V}\sum_r B_T^{(r)} n_i^{(r)} n_j^{(r)} A^{(r)}, \quad (3)$$

$$\beta_{ijkl} = \frac{1}{V}\sum_r \left(B_N^{(r)} - B_T^{(r)}\right) n_i^{(r)} n_j^{(r)} n_k^{(r)} n_l^{(r)} A^{(r)}, \quad (4)$$

where $B_N^{(r)}$ and $B_T^{(r)}$ are the normal and shear compliances of the r th crack in volume V, $n_i^{(r)}$ is the i th component of the normal to the crack, and $A^{(r)}$ is the area of the crack. $B_N^{(r)}$ characterizes the displacement jump normal across the crack produced by a normal traction, while $B_T^{(r)}$ characterizes the shear displacement jump produced by a shear traction. The cracks are assumed to be rotationally symmetric, that is, $B_T^{(r)}$ is assumed to be independent of the direction of the shear traction within the plane of the crack. In equations (1)-(4), the cumulative effect of many cracks is assumed to be additive. In other words, interaction between cracks is neglected (so-called non-interactive approximation, which is valid for a dilute concentration of cracks).

Effect of stress on crack density

To model closure of cracks due to application of anisotropic stress, we can assume that $B_N^{(r)}$ and $B_T^{(r)}$ are the same for all orientations of cracks, while $A^{(r)}$ (and specific area of cracks $s = A^{(r)}/V$) varies with direction of the crack normal, depending on the normal stress acting in that direction,

$$s = s^0 \exp\left(\sigma_n / P_c\right), \quad (5)$$

where s^0 is specific area of all the cracks before application of anisotropic stress, $\sigma_n = \sigma_{ij} n_i n_j$ is normal stress traction acting on the crack surface, and P_c is a characteristic crack closing pressure (Schoenberg, 2002; Shapiro, 2003; Shapiro and Kazelow, 2005; Vlastos et al., 2006). When normal stresses are small compared to P_c, exponential expression in equation 5 can be approximated by a linear expression

$$s = s^0\left(1 + \sigma_n / P_c\right), \quad (6)$$

For uniaxial stress applied along x_1 axis, we have

$$\sigma_{ij} = \sigma_0 \delta_{i1}\delta_{j1}, \quad (7)$$

so that

$$\sigma_n = \sigma_0 n_1^2 = \sigma_0 \cos^2 \vartheta \quad , \quad (8)$$

and

$$s = s^0\left(1 + b\cos^2\vartheta\right), \quad (9)$$

where ϑ is the angle between the crack normal and x_1 axis, and $b = \sigma_0 / P_c$ is normalised stress magnitude.

Evaluation of crack compliance tensors

To calculate tensors α_{ij} and β_{ijkl}, it is convenient to adopt a spherical coordinate system with the polar axis x_i (since both tensors are symmetric with respect to their indexes, we can assume that i is the smallest index) and with transverse angle ϕ measured from any axis which is neither x_i nor x_1. Note that so chosen coordinate system will be different for different components of the tensors. Then, tensor α_{ij} can be written

$$\alpha_{ij} = \frac{B_T}{4\pi}\iint s(\vartheta) n_i n_j \, d\Omega = \frac{Z_{T0}}{4\pi}\iint\left(1 + b n_1^2\right) n_i n_j \, d\Omega, \quad (10)$$

where $i, j = 1,...3$, $d\Omega$ is a body angle element and $Z_{T0} = s_0 B_T$.

A similar approach can be used to evaluate fourth-rank tensor β_{ijkl}. For uniaxially stressed material, all components $i \neq j$ or $k \neq l$ vanish, and the remaining components can be written

$$\beta_{iijj} = \beta_{ij} = \frac{B_N - B_T}{4\pi}\iint s(\vartheta) n_i^2 n_j^2 \, d\Omega \quad (11)$$

or

$$\beta_{iijj} = \beta_{ij} = \frac{Z_{N0} - Z_{T0}}{4\pi}\iint\left(1 + b n_1^2\right) n_i^2 n_j^2 \, d\Omega \quad (12)$$

with $i, j = 1...3$ and $Z_{T0} = s_0 B_T$; in the 4-index version β_{iijj} no summation is implied, while two-index β_{ij} version refers to 6×6 notation. The remaining non-vanishing components of the 6×6 matrix are (Sayers, 2002) $\beta_{44} = \beta_{23}$, $\beta_{55} = \beta_{66} = 4\beta_{12} = 4\beta_{13}$. The resulting matrix β_{ij} can be split into isotropic and anisotropic parts (marked with superscripts *is* and *an* respectively).

$$\beta = \left(Z_{N0} - Z_{T0}\right)\left(\beta^{is} + \beta^{an} b\right). \quad (13)$$

Similarly, for tensor $\bar{\alpha}$,

$$\bar{\alpha} = Z_{T0}\left(\alpha^{is} + \alpha^{an} b\right). \quad (14)$$

A model for stress-induced anisotropy

Elasticity tensors and anisotropy parameters

Then, the equation (1) for the overall compliance tensor can be written in the form

$$S = S^0 + \Delta S^{is} + \Delta S^{an} b \qquad (15)$$

where

$$\Delta S^{is} = Z_{T0}\alpha^{is} + \left(Z_{N0} - Z_{T0}\right)\beta^{is} \qquad (16)$$

is excess compliance contribution of the original (isotropic) distribution of cracks in the unstressed rock and

$$\Delta S^{an} = Z_{T0}\alpha^{an} + \left(Z_{N0} - Z_{T0}\right)\beta^{an} \qquad (17)$$

is excess compliance contribution of cracks created (or closed) due to application of the anisotropic stress. To isolate the effect of anisotropic stress, we rewrite equation (15) in the form

$$S = S^{is} + \Delta S^{an} b \qquad (18)$$

with $S^{is} = S^0 + \Delta S^{is}$ defining the (isotropic) compliance of the unstressed rock. From this tensor, we can estimate anisotropy parameters (Thomsen, 1986; Tsvankin, 1997)

$$\varepsilon = \frac{S_{11}S_{33} - S_{13}^2 - S_{33}^2 + S_{23}^2}{2\left(S_{33}^2 - S_{23}^2\right)}, \quad \gamma = \frac{S_{66} - S_{44}}{2S_{44}}, \qquad (19)$$

and

$$\delta = \frac{\left(S - S_{66}S_{13}\right)^2 - \left(S_{66}\left(S_{33} + S_{23}\right) - S\right)^2}{2S_{66}\left(S_{33} + S_{23}\right)\left(S_{66}\left(S_{33} + S_{23}\right) - S\right)} \qquad (20)$$

with $S = S_{11}\left(S_{33} + S_{23}\right) - 2S_{23}^2$. Retaining only the leading (linear) terms in small parameter $b = \sigma_0 / P_c$, we obtain

$$\varepsilon = \delta = \frac{2}{105}\frac{2\nu B + 6B - 2\nu + 1}{1 - \nu}\mu Z_{T0}\sigma_0 / P_c, \qquad (21)$$

$$\gamma = \frac{1}{105}\left(3 + 4B\right)\mu Z_{T0}\sigma_0 / P_c, \qquad (22)$$

where μ and ν are shear modulus and Poisson's ratio of the unstressed (host) rock, and $B = Z_{N0}/Z_{T0} = B_N/B_T$ is the ratio of normal to tangential compliances of individual cracks. Thus we see that to the first order in applied stress, expressions for ε and δ are identical. This shows that anisotropic crack closure yields elliptical anisotropy, regardless of the value of the compliance ratio B. More precisely, we have shown analytically that if application of small uniaxial stress results in P-wave anisotropy (ellipticity) ε and unellipticity $\varepsilon - \delta$, then

$$\lim_{\varepsilon \to 0}\frac{\varepsilon - \delta}{\varepsilon} = 0. \qquad (23)$$

for any values of the compliance ratio B and host rock's Poisson's ratio ν.

Figure 1a,b shows anisotropy parameter ε and ratio ε / γ versus Poisson's ratio ν for different values of compliance ratio *B*. The same data plus anisotropy parameter γ are replotted in Figure 2a,b as functions of *B* for different values of ν. One important thing about these plots is that they are *not* examples: plots 1b and 2b are completely universal. Plots 1a and 2a are universal subject to change of vertical scale according to the magnitude of applied stress. Of course, the results are restricted to small stresses and the resulting weak anisotropy.

In these plots it is assumed that the shear modulus of the unstressed rocks is the same. If we instead assume constant bulk modulus or, say, constant compressional velocity, the dependency on Poisson's ratio would be somewhat different. However it is clear that the anisotropy parameters only mildly depend on Poisson's ratio in a range typical for dry consolidated rocks (say, 0.1-0.3).

In Figure 2b, we also show (as circles) the values of ε / γ ratio for uniaxial stress and uniaxial strain experiments on Berea sandstone reported by Scott and Abousleiman (2004). These values plot near the *B*=0.4 line, which is within typical range for sandstones (Sayers, 2002, Gurevich et al., 2009). This is despite the fact the anisotropy reported by these authors is not weak and significantly deviates from ellipticity, particularly for the uniaxial stress experiment. Possible causes of this are rock damage under non-hydrostatic stress (confirmed by strong acoustic emissions) and resulting heterogeneity of the sample, as well difficulties in accurately measuring ultrasonic velocities at oblique angles of incidence.

Discussion and conclusions

The result concerning ellipticity of stress-induced anisotropy is consistent with a generally proven fact that anisotropy arising from application of anisotropic stress to an isotropic nonlinearly elastic medium is always elliptical (see Rasolofosaon, 1998). Note that this is also true for anisotropy caused by application of uniaxial *strain*, because the state of stress corresponding to a uniaxial strain can be achieved by a combination of an isotropic stress and a uniaxial stress.

At the same time, it is known that an isotropic medium permeated by a set of aligned identical fractures is elliptical if and only if the fractures are scalar, that is, their compliance ratio $B = Z_N/Z_T$ is 1. A number of experimental and theoretical studies suggest that for real fractures, parameter *B* is most often significantly smaller than 1. Typical values are between 0.3 and 0.6 (Biwa et al., 2005; Baltazar et al., 2002). This opens the possibility of differentiating between stress- and fracture-induced

azimuthal anisotropy by estimating the degree of unellipticity. Conversely, if the cause of anisotropy is known, then the patterns discussed above allow one to estimate *P*-wave anisotropy from *S*-wave anisotropy, by assuming or measuring a value of parameter B.

The above analysis is valid for dry rocks but not for fluid-saturated rocks (unless the cracks are hydraulically isolated). For interconnected cracks at sufficiently low frequencies, the effect of fluid saturation can be computed using anisotropic Gassmann equations (Brown and Korringa, 1975; Gurevich, 2003). For higher frequencies, dispersion due to wave-induced flow between cracks and pores may need to be taken into account. Flow between compliant grain contacts and equant pores can be modelled with one of the known squirt flow models. Flow associated with larger-scale fractures can be modelled using a mesoscopic model based on the theory of poroelasticity (Gurevich et al., 2009). It can be shown that if the dry medium is elliptical, the saturated medium is also elliptical, and this ellipticity holds for all frequencies. In contrast, unellipticity of the fluid-saturated medium with aligned fractures will deviate from that of the dry medium and will vary with frequency (with the largest unellipticity attained in the high-frequency limit, where $B \approx 0$). However, these variations are not large enough to blur the distinction between stress- and fracture-induced anisotropy.

Acknowledgements

We thank Colin Sayers, Serge Shapiro and Joel Sarout for useful discussions. BG thanks Curtin Reservoir Geophysics Consortium for financial support.

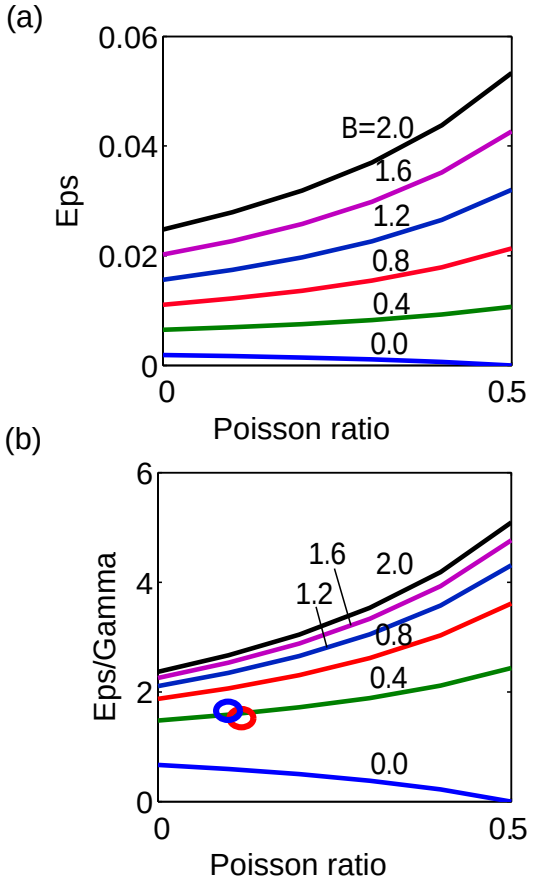

Figure 1: Anizotropy parameter ε (a) and ratio ε/γ (b) as functions of Poisson ratio for different vaues of compliance ratio *B*.

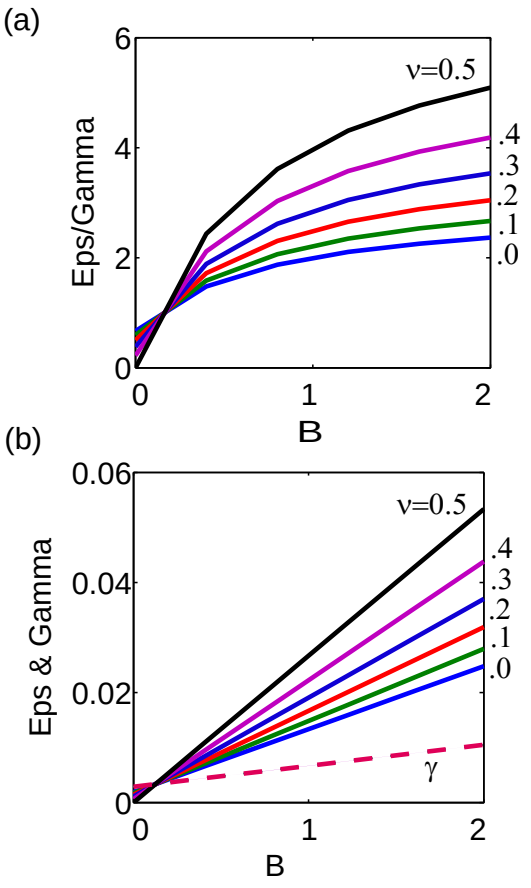

Figure 2: Anizotropy parameters ε and γ (a) and ratio ε/γ (b) versus Poisson ratio for different vaues of compliance ratio *B*.

EDITED REFERENCES

Note: This reference list is a copy-edited version of the reference list submitted by the author. Reference lists for the 2010 SEG Technical Program Expanded Abstracts have been copy edited so that references provided with the online metadata for each paper will achieve a high degree of linking to cited sources that appear on the Web.

REFERENCES

Angus, D. A., J. P. Verdon, Q. J. Fisher, and J.-M. Kendall, 2009, Exploring trends in microcrack properties of sedimentary rocks: An audit of dry-core velocity-stress measurements: Geophysics, **74**, no. 5, E193–E203.

Gurevich, B., Makarynska, D. and Pervukhina, M., 2009, Are penny-shaped cracks a good model for compliant porosity? 79th Annual International Meeting, SEG, Expanded Abstracts, 3431–3435.

Mavko, G., T. Mukerji, and N. Gofrey, 1995, Predicting stress-induced velocity anisotropy in rocks: Geophysics, **60**, 1081–1087.

Nur, A., 1971, Effects of stress on velocity anisotropy in rocks with cracks: Journal of Geophysical Research, **76**, 2022–2034.

Rasolofosaon, P., 1998, Stress-induced seismic anisotropy revisited: Proceedings of the 8th International Workshop on Seismic Anisotropy (8IWSA), **53**, no. 5, 679–692.

Sayers, C. M., 2002, Stress-dependent elastic anisotropy of sandstones: Geophysical Prospecting, **50**, 85–95.

Sayers, C., and D.-H. Han, 2002, The effect of pore fluid on the stress-dependent elastic wave velocities in sandstones: 72nd Annual International Meeting, SEG, Expanded Abstracts, 1842–1845.

Sayers, C., and M. Kachanov, 1995, Microcrack-indused elastic wave anisotropy of brittle rock: Journal of Geophysical Research, **100**, 4149–4156.

Schoenberg, M, 2002, Time-dependent anisotropy induced by pore pressure variation in fractured rock: Journal of Seismic Exploration, **11**, no. 1-2, 83–105.

Scott, T. E., and Y. Abousleiman, 2005, Acoustic measurements of the anisotropy of dynamic elastic and poromechanics moduli under three stress/strain pathways: Journal of Engineering Mechanics, **131**, no. 9, 937–946.

Shapiro, S. A., 2003, Elastic piezosensitivity of porous and fractured rocks: Geophysics, **68**, 482–486.

Shapiro, C. A. and A. Kaselow, 2005, Porosity and elastic anisotropy of rocks under tectonic-stress and pore-pressure changes: Geophysics, **70**, no. 5, 27–38.

Thomsen, L., 1986, Weak elastic anisotropy: Geophysics, **51**, 1954–1966.

Tsvankin, I., 1997, Anisotropic parameters and P-wave velocities for orthorhombic media: Geophysics, **62**, 1292–1309.

Vlastos, S., E. Liu, I. G. Main, M. Schoenberg, C. Narteau, X. Y. Li, and B. Maillot, 2006, Dual simulations of fluid flow and seismic wave propagation in a fractured network: effects of pore pressure on seismic signature: Geophysical Journal International, **166**, 825–838.